2023 年臺灣國際科學展覽會
優勝作品專輯

作品編號 160040

參展科別 物理與天文學

作品名稱 Development of UV-Protection Roofing Tile from Nitrogen-doped Graphene Quantum Dots (N-GQDs) for Rubber Drying Chambers

得獎獎項 四等獎

國　　家 Thailand

就讀學校 Princess Chulabhorn Science High School Pathum Thani

指導教師 Khunthong Klaythong

Boonchoat Paosawatyanyong

作者姓名 Wallapha Phatrabuddhikul

Siriya Mektavepong

Supakorn Kajornkiatinukul

關鍵詞 rubber sheet、drying chamber、N-GQDs roof

作者照片

Abstract

Improved methods of processing latex into rubber sheets will improve the incomes of small rubber producers. There are two ways in which latex can be processed into rubber sheets: fumigation and solar incubation. The fumigation method is expensive and produces pollution, but solar incubation can cause dark, sticky rubber sheets due to UV radiation, which reduces their value. A low-cost and environmentally-friendly solution to this problem was investigated here. A UV-protective roofing panel made using Nitrogen-doped Graphene Quantum Dots (N-GQDs) was developed and tested. N-GQDs were made using the hydrothermal process for 2 and 4 hours (T2 and T4) and the solvothermal process for 4, 6, and 8 hours (TS4, TS6, and TS8). It was found that all types of N-GQDs absorbed light in the UV range, withT4 showing the greatest absorption. T4 had the greatest Fluorescent Intensity (FL) value, emitting blue light, while for the solvothermal method TS6 had the highest FL value, emitting red light. T4 and TS6 were chosen for further testing, and were applied to a clear roofing tile. After installing the roof on the chamber, the temperature inside was higher than outside. Then we measure the UV protection efficiency of the roof which was 93.27%. The average temperature was 45^{o}C, which is the temperature for drying rubber sheets. Due to the roof's capability to absorb UV radiation and heat the chamber, our N-GQDs roof has a great ability to produce higher-quality rubber sheets.

Introduction

Thailand is the world's major rubber producer. Thai rubber plantation farmers still prefer to convert fresh latex to raw rubber sheets because most Thai rubber plantations are small plantations. There is not much productivity. Most of the rubber often processed into raw rubber sheets to be sold to merchants or fumigation factories. It also solved the problem of falling para rubber prices, which caused the Thai para rubber production structure to produce more rubber sheets than other rubber. (Kampan, 2017)

The processing of raw rubber latex into rubber sheets can be done in two ways: by fumigating raw rubber sheets or by drying raw rubber sheets. For the fumigation of raw rubber sheets, the cost of firewood is high, and heat loss is typically high. The second method, drying by solar incubation, can be considered a clean energy alternative that is not toxic to the environment and has unlimited renewable power. (Aguele et al., 2015) However, existing incubators often encounter problems with the formation of sticky and dark rubber sheets due to exposure to UV radiation, which reduces the value. One solution to the problem of UV damage is to use polycarbonate roofing tiles, but polycarbonate is slow to degrade, leading to long-term plastic waste issues. (Bacon et al., 2013)

Nitrogen-doped graphene quantum dots (N-GQDs) are particles having low biotoxicity and fluorescence properties. These particles can absorb most radiation in the UVB range, and the wavelengths of light emitted by Graphene Quantum Dots (GQDs) cover the entire visible light spectrum and the red spectrum (Sk et al., 2014). The efficiency of GQDs can be improved by coating them with nitrogen, called Nitrogen-doped Graphene Quantum Dots (N-GQDs), which was found to increase the fluorescence quantum yield, or fluorescence efficiency, by up to 94% (Qu et al., 2014). The efficiency of GQD particles as a fluorescent agent capable of absorbing UV radiation makes them effective as a particle for UV protection. (Purcell-Milton & Gun'ko, 2012) The low-cost methods for synthesizing N-GQDs are hydrothermal and solvothermal which use different solvents. The hydrothermal method uses water as a solvent and the solvothermal method uses acid as a solvent. (Gu et al., 2016)

Here, we develop and test the effectiveness of N-GQD-coated UV-protective roofing for rubber sheet drying plants to produce high-quality rubber sheets according to ASTM D882 standards which is the standard for testing physical properties of the polymer. The N-GQDs roofing dryer also uses clean energy that is not toxic to the environment and is renewable energy. This allows farmers to reduce their energy costs while producing higher quality rubber. For this reason, UV-protective N-GQD-coated roofing tiles may help to increase the country's potential in rubber sheet exports as well as the income of rubber farmers.

Questions, Variables, and Hypothesis

Questions

How can we improve the quality of rubber sheets along with decreasing pollution in a global environment?

1. To what extent do different durations for the synthesis of N-GQDs by hydrothermal method affect the wavelengths absorbed and emitted by the N-GQDs?
2. To what extent do different durations for the synthesis of N-GQDs by the solvothermal method affect the wavelengths absorbed and emitted by the N-GQDs?
3. To what extent does the roof from N-GQDs meet the ASTM D882 standard physical properties?
4. To what extent does the roof from N-GQDs effective in defending UV light?
5. To what extent does the roof from N-GQDs effective in retaining heat in rubber drying chamber?

Variables

Part 1: Study of the wavelengths absorbed and emitted by N-GQDs when using different hydrothermal synthesis periods.

<u>Independent Variables</u>: Hydrothermal synthesis periods
<u>Dependent Variables</u>: The wavelength absorbed and emitted by N-GQDs
<u>Control Variables</u>: Reactant quantity, synthesis temperature, synthesis vessel

Part 2: Study of the wavelengths absorbed and emitted by N-GQDs when using different solvothermal synthesis periods.

<u>Independent Variables</u>: Solvothermal synthesis periods
<u>Dependent Variables</u>: The wavelength absorbed and emitted by N-GQDs.
<u>Control Variables</u>: Reactant quantity, synthesis temperature, synthesis vessel

Part 3: Studying the physical properties of N-GQDs roof with ASTM D882.

<u>Independent Variables</u>: N-GQDs roof
<u>Dependent Variables</u>**:** The physical properties of N-GQDs roof.
<u>Control Variables</u>**:** Sample size, test speed, instrumentation test

Part 4: Study of the UV-protection efficiency of N-GQDs roof

<u>Independent Variables:</u> N-GQDs roof
<u>Dependent Variables:</u> percentage of UV light passing N-GQDs roof
<u>Control Variables:</u> size of N-GQDs roof, initial amount of UV light

Part 5: Study of the heat storage efficiency of rubber drying chamber from N-GQDs roof.

<u>Independent Variables:</u> rubber drying chamber from N-GQDs roof
<u>Dependent Variables:</u> temperature difference inside the chamber and outside the chamber
<u>Control Variables:</u> Duration, test date, instrumentation test

Hypothesis

1. Different synthesis durations in the hydrothermal method affect the wavelengths absorbed and emitted by N-GQDs.
2. Different synthesis durations in the solvothermal method affect the wavelengths absorbed and emitted by N-GQDs.
3. N-GQDs roof has high physical properties according to ASTM D882 standard.
4. N-GQDs roof has high UV-protection efficiency.
5. Rubber drying chambers with N-GQDs roofs have high heat storage efficiency.

Background Research

1. Rubber

1.1 Latex characteristics

Natural rubber is chemically known as cis-1,4-polyisoprene. The side chain group of rubber, polyisoprene, has very small electronegativity, making natural rubber not resistant to oil and giving it good electrical insulation. Moreover, natural rubber is also not resistant to UV radiation and ozone. The molecules are mixed in natural rubber latex, which resembles a milk-like white liquid because it is a colloid (Mastalygina et al., 2020).

1.2 The raw rubber sheet

The raw rubber sheet is latex which goes through air and heat. A good quality rubber sheet is a flexible, clean rubber sheet with a uniform color and a standard size of 38-46 cm wide and 80-90 cm long, with a thickness of 3–4 mm. The good quality rubber increases the price of the rubber sheet. (Marlina & Adi Prasetya, 2017)

2. Solar drying method

An important problem with the limitation of solar rubber sheet curing is that the UV radiation present in the sun will result in the deterioration of the rubber sheet quality (ITOH et al., 2006). There are three types of UV color in sunlight: UVA has a wavelength of 320-400 nm, UVB has a wavelength of 280-320 nm, and UVC has a wavelength of 100-280 nm. The Earth intercepts it before it reaches the Earth's surface. Only UVA and UVB are left to penetrate the Earth's atmosphere and reach the Earth's surface, where UVA is up to 95% (Repacholi, 2000).

3. Quantum Dots

Quantum dots are nanoparticles with unique fluorescent characteristics (Sk et al., 2014). Quantum dots absorb light, then emit light at lower wavelengths. This feature has attracted a wide range of applications, such as cell imaging. The emission spectra of quantum dots can be controlled by the particle size. When the particle size is large, the longer the wavelength emitted (Purcell-Milton & Gun'ko, 2012).

Normally, quantum dots contain cadmium and others heavy metal, which is toxic to living organisms. Therefore, graphene quantum dots, which is based on carbon, was developed. It is water-soluble and non-toxic. The wavelengths emitted by graphene quantum dots are in the range of 235.2–995.5 nm (Sk et al., 2014). The main difference between graphene quantum dots and other types of quantum dots is the wide energy band range. This allows light emission to reach the red wavelength region (Bacon et al., 2013). Nitrogen coated on quantum dot (N-GQDs) to increase the fluorescent quantum yield (FL). According to the work of Dan Qu et al. up to 94% of the quantum graphene coating was achieved (Gu et al., 2016).

4. Polyvinyl alcohol; PVA

PVA is partially crystalline from its formation and is characterized by properties such as chemical resistance, water solubility, and biodegradability (Mok et al., 2020). PVA is chemically bound or physically entangled with nanoparticle surfaces (Guo et al., 2009) and common polymers used. Due to special chemical and physical properties, it is widely used as a substrate material, which should be used on land or away from the water surface (Kamoun et al., 2015), for example, over a large area, where it may be used as a film or adhesive (Ghebaur et al., 2012). Biocompatibility It is resistant to temperature and solar changes and is non-toxic to the environment and humans (Liu et al., 2007).

5. ASTM D882 standard

It is a standard designed specifically for the testing of plastics less than 1 mm thick and can be used to test any plastic specimen within this thickness range.

The test in this standard is for specimens with a thickness not exceeding 10% of the specimen length between the specimen holders. The specimen should not exceed 1 mm in thickness and be between 5.0 and 25.4 mm in width. The length of the test specimen is 100 mm–250 mm (Pryor, n.d.).

Materials List

1. Materials

1) PVC pipe
2) Square mold 0.5 x 0.5 m^2
3) metal angle bar 0.5 m

2. Equipments

1) teflon lined autoclave
2) Beaker
3) glass rod
4) measuring cylinder
5) UV meter

3. Tools

1) Thermal oven (UN55, Memmert)
2) Digital scale (Scout Pro, OHAUS)
3) UV/VIS Spectrophotometer (T60, PG INSTRUMENTS)
4) Fluorescence Spectrophotometer (F-4600, HITACHI)
5) Thermometer (MS6531A, MASTECH)
6) Tensile tester (KJ-10858, KINSGEO)
7) Overhead stirrer (OS40-S, DRAGON LAB)

4. Chemical

1) Citric acid ($C_6H_8O_7$)
2) Sulfuric acid (H_2SO_4)
3) Deionized water (H_2O)
4) Urea ($CH_4N_2O_2$)
5) Poly vinyl alcohol $(CH_2CH)_n$

Experiment Procedure

1. Synthesis and spectroscopy of the N-GQDs

Hydrothermal N-GQDs were synthesized by adding 2.1 g of citric acid and 1.8 g of urea to 50 ml of deionized water and stirring until the solution fully dissolved, then heating at 160^{o}C for 2 and 4 hours. (T2 and T4, respectively). A UV/VIS spectrophotometer was then used to observe the wavelengths absorbed by T2 and T4. Finally, the spectrum emitted by a Fluorescence Intensity (FL) spectrophotometer using excitation wavelengths ranging from 250 to 375 nm was observed.

Solvothermal N-GQDs were synthesized by adding 2.1 g of citric acid and 1.8 g of urea in 50 ml of 7.4 M sulfuric acid and stirring until the solution fully dissolved, then heating at 210^{o}C for 4, 6, and 8 hours. (TS4, TS6, and TS8, respectively). The UV/VIS spectrophotometer was then used again, and the FL spectrophotometer was used for wavelengths ranging from 250 to 425 nm which are the range of UV light.

2. Making and testing of N-GQDs roofing tiles

T4, which absorbs light at the widest spectrum and has the highest FL, and TS6, which emits the highest wavelength and has the greatest FL, were chosen for further testing. 125 ml of each solution was mixed with 10 g of polyvinyl alcohol (PVA), then heated at 60^{o}C with constant stirring for 2 hours.

The solution was then poured into 10 x 10 cm^2 and 50 x 50 cm^2 acrylic molds and allowed to cool until it forms a solid sheet. The sheet formed from PVA containing T4 is called P-UV and TS6 is called P-IR. The 10 x 10 cm^2 sheets were cut into 5 pieces of 2 x 10 cm^2 and tested with an ASTMD882 standard Tensile Tester.

3. UV-protection and heating efficiency of N-GQDs roofing tiles

One sheet each of 50 x 50 cm^2 P-UV (on top) and 50 x 50 cm^2 P-IR were layered to form a roof structure which was place in direct sunlight. A UV meter was used to measure UV intensity at 12:00 pm directly above and below the roof at 5 points on the roof for 7 days, as shown in figure 1. A drying chamber with dimensions 0.5 x 0.5 x 0.5 m^3 was built with the same 2-layer P-UV/P-IR roof design, and placed outside. Temperature measurements inside and outside the chamber were made for 7 days at 8:00, 12:00, and 16:00, as shown in figure 2.

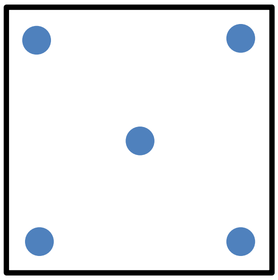

Figure 1 spots of UV intensity measurement on N-GQDs roof

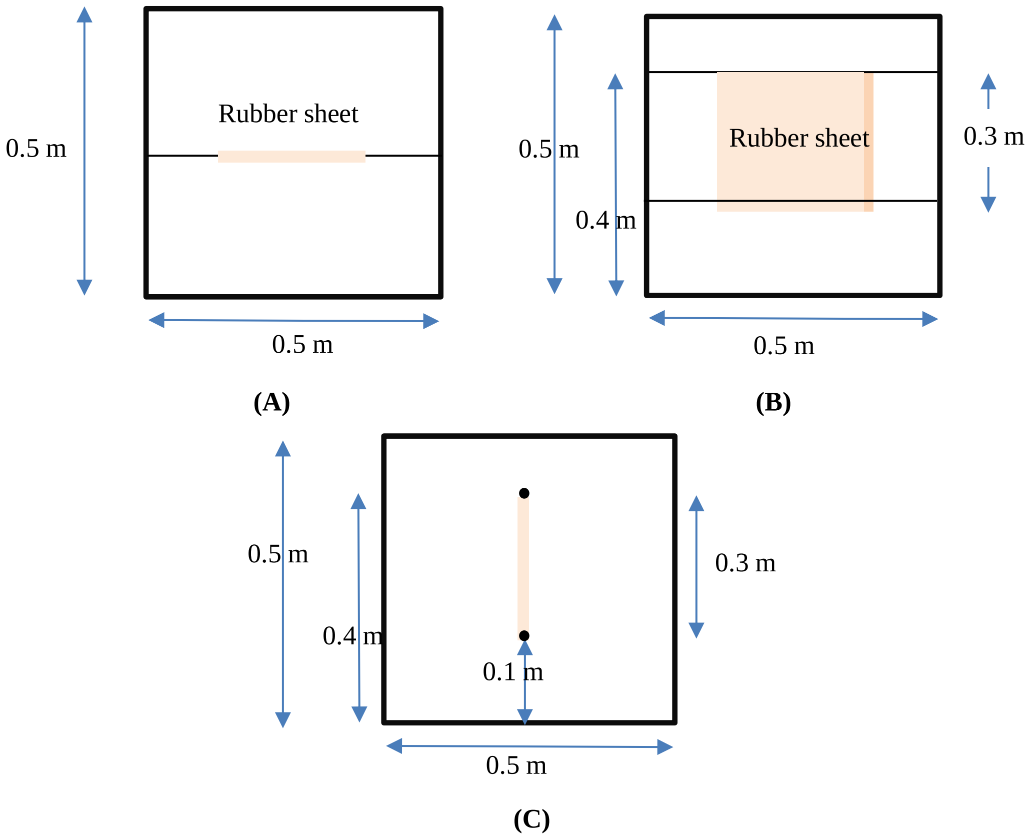

Figure 2 drying chamber (A) Top view (B) Front view (C) Side view

Data Analysis and Discussion

1. <u>The spectroscopy of N-GQDs for different hydrothermal synthesis periods</u>

Graph 1 shows the absorbance of N-GQDs (T2 and T4)

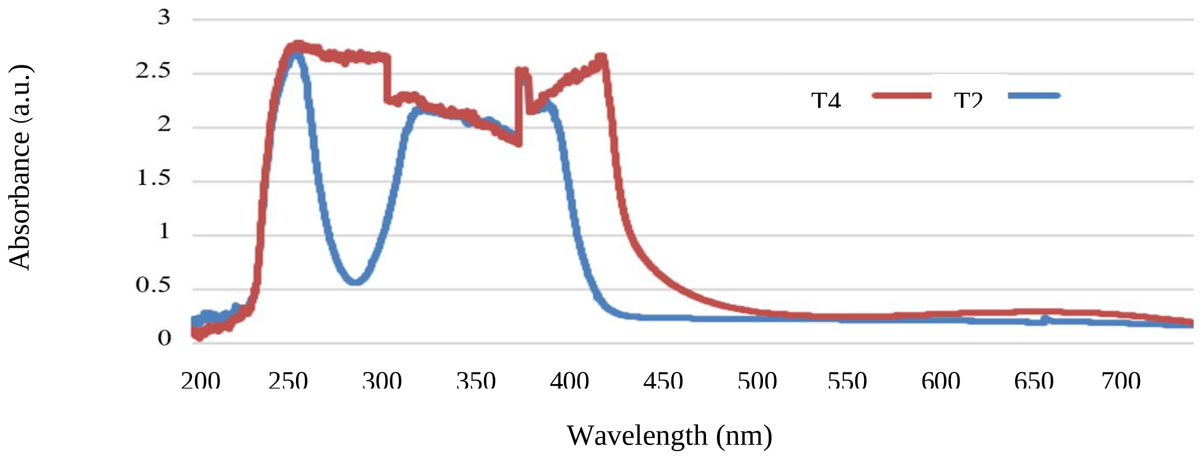

Graph 2 (a) shows the emission spectrum of T2; (b) shows the emission spectrum of T4

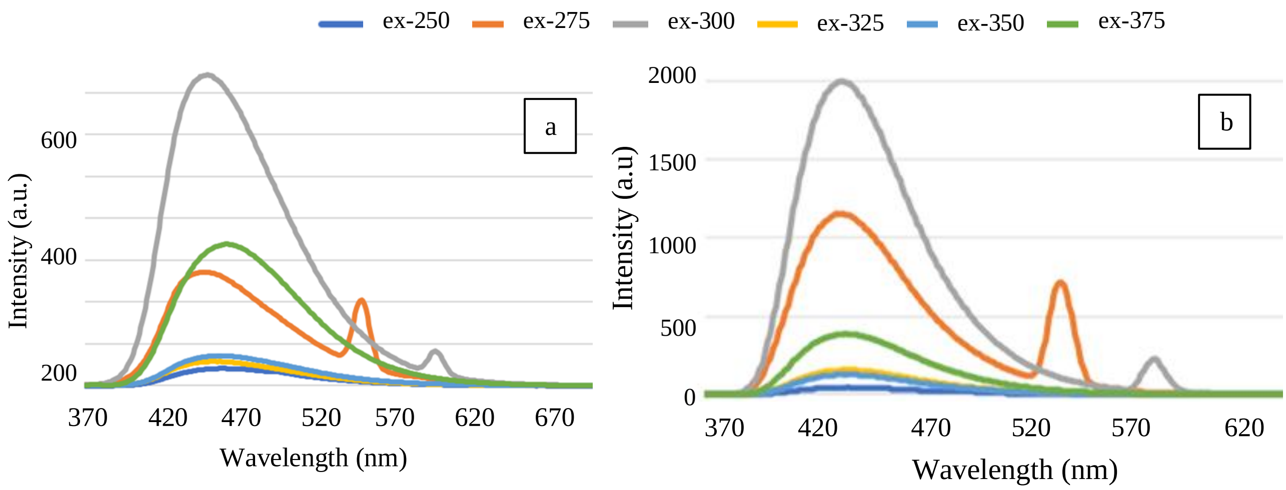

Graph 1 shows that T2 and T4 absorbed light in the UV range. The graph also shows that T4 had the wider absorbance range, while T2 had the greatest absorbance at 364 nm and 250 nm, T4 had the greatest absorbance at 401.4 nm, 363.8 nm, 289.6 nm, and 253.6 nm.

This is because the bandgap size, or energy band, of N-GQDs, is approximately 4 eV, and the particles do not absorb light with lower energies than the energy band. The energy of UV light is 3–124 eV, allowing the N-GQD particles to absorb light in the UV range.

Graph 2 (a) shows that T2 had the highest fluorescence intensity (FL) stimulated by 300 nm light with maximum FL at 452 nm. Graph 2 (b) shows that T4 had the highest FL stimulated by 300 nm light with a maximum FL 438 nm. In comparison, FL values of T4 were higher.

The synthesis time of N-GQDs affects the particle size (Papaioannou et al., 2019), If the particles are too large, the optical properties of N-GQDs are also reduced. From the experimental results, it was seen that the 2-hour synthesis time had lower FL values than the 4-hour synthesis (Gu et al., 2016).

2. <u>The spectroscopy of N-GQDs for different solvothermal synthesis periods</u>

Graph 3 shows the absorbance of the synthetic N-GQDs at 4, 6, and 8 hours (TS4, TS6, and TS8 respectively).

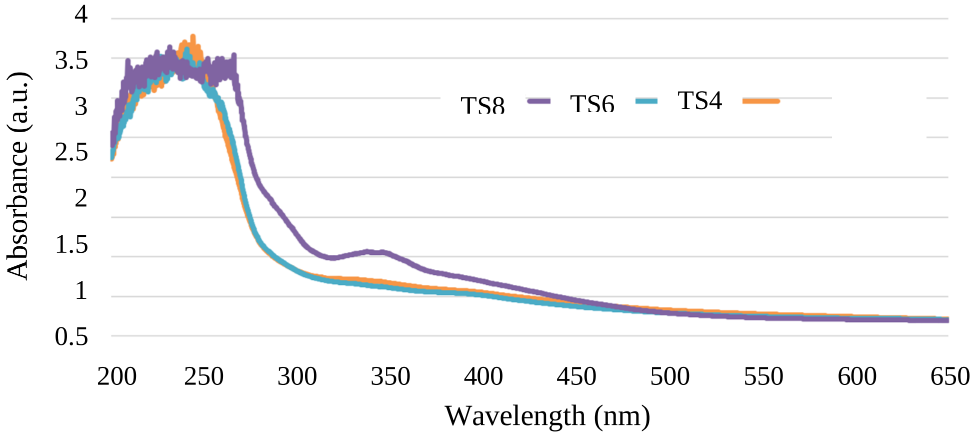

Graph 4 shows the emission of synthetic N-GQDs at 4 hours (TS4), excitation light at different wavelengths

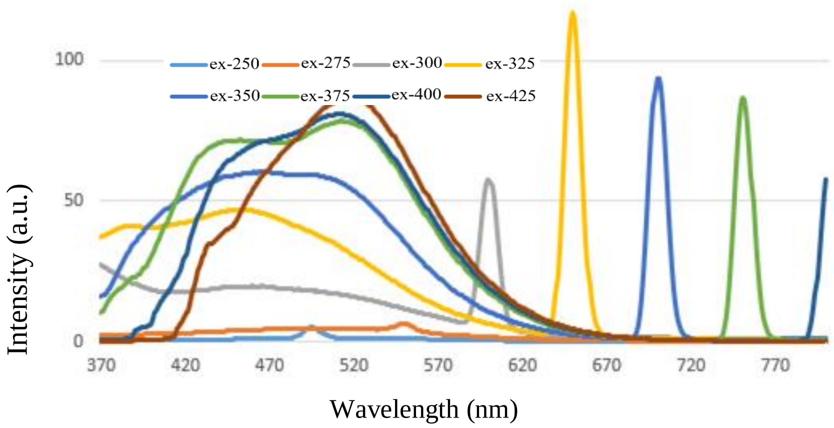

Graph 5 shows the emission of synthetic N-GQDs at 6 hours (TS6) excitation light at different wavelengths

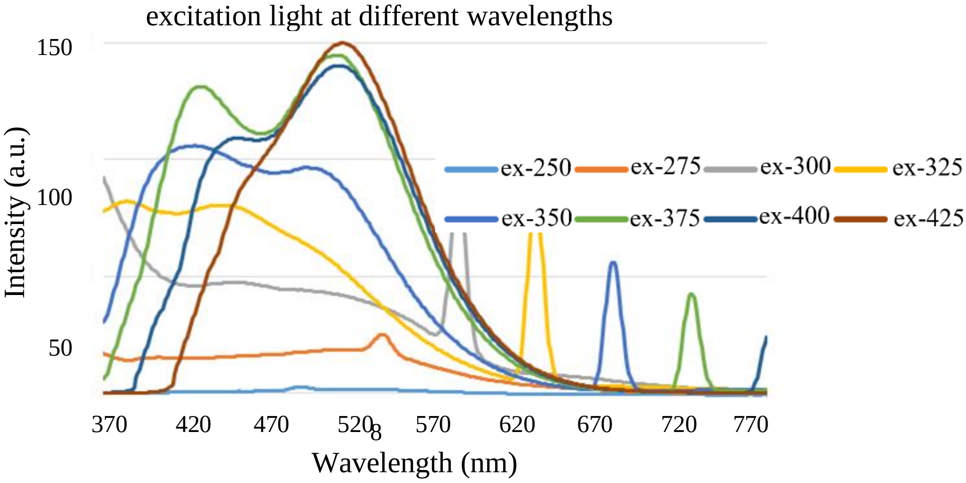

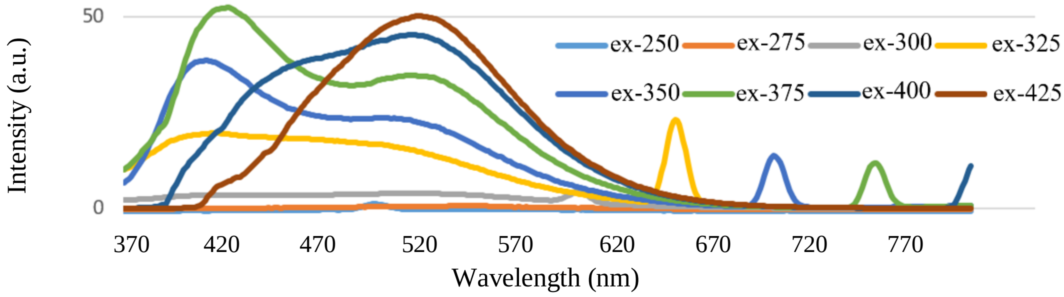

Graph 6 shows the emission of synthetic N-GQDs at 8 hours (TS8), with excitation light at different wavelengths

Graph 3 shows that TS4, TS6, and TS8 had the greatest absorbance in the UV range, with TS4 having the greatest absorbance at 243.8 nm. TS6 had the greatest absorbance at 245 nm, and TS8 had the highest absorbance at 252 nm.

Graph 4 shows that when TS4 is stimulated at a wavelength of 425 nm, it had a peak FL value at a wavelength of 519 nm. Graph 5 shows that when TS6 is stimulated at a wavelength of 425 nm, it had a peak FL value at a wavelength of 525 nm. Graph 6 shows that when TS8 is excited at a wavelength of 375 nm, it had a peak FL value at a wavelength of 422 nm. Red light was emitted by all three conditions, but TS6 had the highest FL.

Solvothermal synthesis uses sulfuric acid as the solvent, which gives a sulfur coating to the N-GQD particles. This reduces the energy band size (Huali Shi et al., 2022), making it only inversely proportional to the absorbed wavelength, which made TS4, TS6, and TS8 absorb light at higher wavelengths than T4 and T6.

The results showed that the synthesis time of 6 hours was the period in which the FL was the highest, which means that this is the most appropriate duration. In addition, TS4, TS6, and TS8 emitted light at higher wavelengths than the hydrothermal synthesis, which uses water as the solvent. This is because the presence of sulfur coating causes the phenomenon of Red Shift, which causes the light emission spectrum of solvothermal synthesized particles to be higher than that of hydrothermally synthesized particles (Liu et al., 2021).

3. <u>The physical properties of N-GQDs roofing tile</u>

Graph 7 shows stress-strain curves for P-IR, P-UV, and PVA

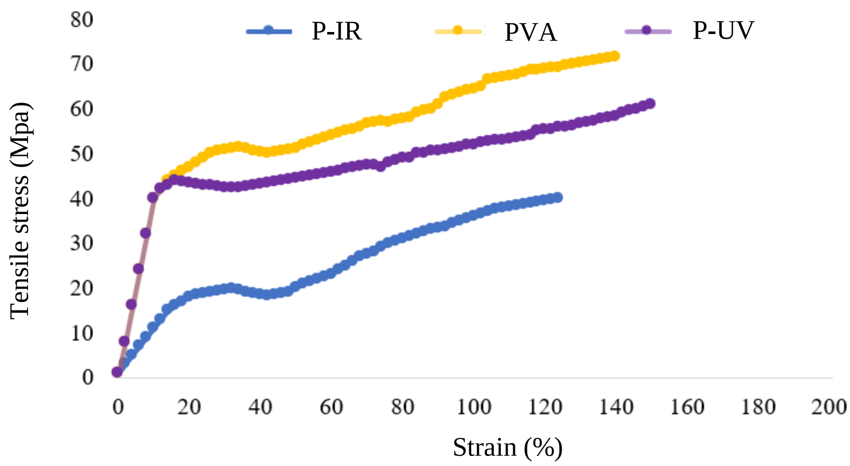

As shown in graph 7, P-IR had the lowest strength and elongation at break, while PVA had the highest. P-UV can be stretched the most at 141% and the least is P-IR at 124%. The tensile strength of P-IR, PVA, and P-IR were 40, 71.5, and 61, respectively.

Since P-IR roofing sheets contain a mixture of sulfuric acid-based N-GQDs, the pH of the solution prior to mixing with PVA is lower than that of P-UV. In 2000, it was reported that acetic acid content affects the structure of the PVA sheet, resulting in a decrease in the thickness of the PVA sheet and an increase in porosity due to the H_3O^+ concentration. As a result, the sulfuric acid-containing P-IR is less resilient than the P-UV roof due to the concentration of H_3O^+ ions, resulting in the sheet being slightly thinner and more porous (Chuang, 2000; Shi et al., 2008). Similarly, P-UV still shows a stress-strain curve comparable to PVA but slightly lower because of the mixture of particles.

4. UV-protection and heating efficiency of N-GQDs roofing tiles

Table 1 shows intensity and percentage of average UV light upper and lower side of PVA roof

Date	Upper side (mW/cm^2)	Lower side (mW/cm^2)	Percentage
1st Day	2.9	2.5	13.7%
2nd Day	3.4	3.0	11.7%
3rd Day	3.7	3.2	13.5%
4th Day	4.1	3.7	9.7%
5th Day	4.1	3.8	7.3%
6th Day	3.3	2.8	15.1%
7th Day	2.8	2.5	10.7%
Average	3.47	3.07	15.2%

Table 2 shows intensity and percentage of average UV light upper and lower side of N-GQDs roof

Date	Upper side (mW/cm^2)	Lower side (mW/cm^2)	Percentage
1st Day	3.1	0.1	96.7%
2nd Day	3.6	0.2	94.4%
3rd Day	3.8	0.3	92.1%
4th Day	4.2	0.4	90.4%
5th Day	4.0	0.3	92.5%
6th Day	3.2	0.2	93.7%
7th Day	2.9	0.3	93.1%
Average	3.54	0.25	93.27%

Table1 shows the UV protection efficiency of PVA roof. According to the table, the average measured at upper and lower side of the roof are 3.47 mW/cm^2 and 3.07 mW/cm^2, respectively. The average UV-protection efficiency of PVA roof is 15.2%.

Table 2 shows the UV protection efficiency of N-GQDs. As can be seen from the table, the average UV measured at upper and lower side of N-GQDs are 3.54 mW/cm^2 and 0.25 mW/cm^2, respectively. On the 4th of experiment, UV measured at upper side of the roof was highest at 4.2 mW/cm^2. When calculated, the highest UV protection efficiency was 96.7%, the lowest was 90.4%, and the average was 93.27%.

Table 3 shows the indoor and outdoor of PVA rubber drying chamber temperatures recorded in 3 time periods for 7 days

Date	8:00		12:00		16:00	
	Temperature inside (°C)	Temperature outside (°C)	Temperature inside (°C)	Temperature outside (°C)	Temperature inside (°C)	Temperature outside (°C)
1st Day	34.3	33.9	39.0	38.5	38.1	36.3
2nd Day	35.2	34.6	40.2	39.1	37.9	36.4
3rd Day	36.0	35.0	40.0	38.8	39.0	36.9
4th Day	35.2	34.0	39.9	39.1	38.5	36.5
5th Day	35.5	34.6	39.5	38.0	39.1	37.0
6th Day	33.6	32.1	38.4	37.5	38.9	37.4
7th Day	35.2	34.5	40.3	39.7	38.7	36.5
Average	35.0	34.1	39.6	38.7	38.6	36.7

Table 4 shows the indoor and outdoor of N-GQDs rubber drying chamber temperatures recorded in 3 time periods for 7 days

Date	8:00		12:00		16:00	
	Temperature inside (°C)	Temperature outside (°C)	Temperature inside (°C)	Temperature outside (°C)	Temperature inside (°C)	Temperature outside (°C)
1st Day	39.3	33.9	47.3	38.5	42.5	36.3
2nd Day	39.8	34.6	47.9	39.1	43.1	36.4
3rd Day	40.2	35.0	48.2	38.8	43.8	36.9
4th Day	38.3	34.0	50.8	39.1	42.6	36.5
5th Day	38.9	34.6	47.0	38.0	44.8	37.0
6th Day	38.6	32.1	45.7	37.5	45.1	37.4
7th Day	39.7	34.5	48.0	39.7	44.8	36.5
Average	39.3	34.1	47.8	38.7	43.8	36.7

Graph 8 shows the difference between the mean temperature outside the chamber and the mean temperature inside the chamber.

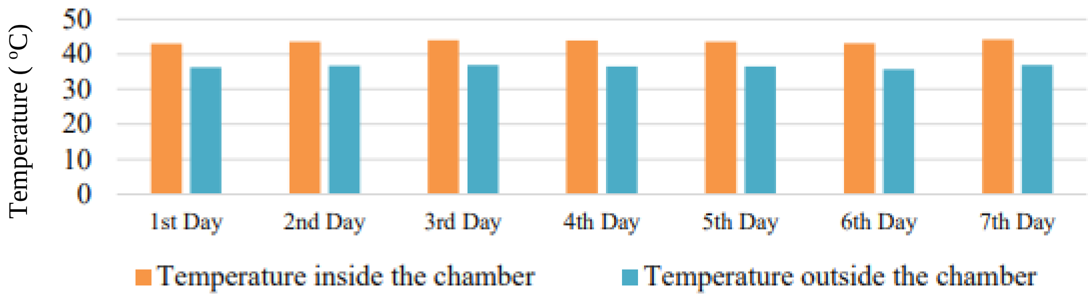

Table 3 shows that the temperature inside the chamber was higher than the temperature outside the chamber. The day with the highest indoor temperatures was on the 7th day at 12:00 at 40.3°C. The averages temperature difference between the inside and outside of the chamber at 8:00 was 0.9°C, at 12:00 was 0.9°C, and at 16:00 was 1.9°C.

Table 4 shows that the temperature inside the chamber was higher than the temperature outside the chamber. The day with the highest indoor temperature was on the 4^{th} day at 12:00 at 50.8°C. The averages temperature difference between the inside and outside of the chamber at 8:00 was 5.2°C, at 12:00 was 9.1°C, and at 16:00 was 7.1°C.

Graph 8 shows that the average temperature inside the chamber was about 43°C, while the temperature outside was around 38°C. The highest average indoor temperature was recorded on the seventh day, at 44.2°C.

Because the absorption spectrum of T4 contained P-UV and the emission spectrum of TS6 contained P-IR, a P-UV layer was applied to the N-GQDs roof to protect the rubber sheets from UV radiation, and a P-IR layer was applied to produce heat in the chamber.

In addition, the amount of UV light varied at different times of the day. When measuring the UV radiation in the chamber at 25 different points, the UV radiation at 12:00 was the highest, followed by 16:00 and 08:00, respectively. This meant that the amount of red light produced by P-IR was different at different times.

Conclusions

From our study, we found that after synthesis, T4 had the highest absorbance in the UVA, UVB, and UVC ranges. In addition, TS6 had the highest FL in the range of red light, which has the most heat among visible light. When the polymer was molded, we found that the P-UV roof from T4 had more strength than the P-IR roof from TS6. After studying heat storage efficiency, we also found that the temperature inside the solar drying chamber was higher than the temperature outside. The average UV protection efficiency of N-GQDs roof was 93.27%. Lastly, the average temperature inside the solar drying chamber was 43°C, which is the most suitable temperature for drying rubber sheets. Finally, we can conclude that our innovation, N-GQDs roofs, can produce high quality rubber sheets for rubber farmers with low-cost and environmentally friendly methods.

Ideas for future research

For further research, we plan to adapt our N-GQDs innovation to urban society to promote UV protection of people's skin or eyes. For example, it could be adapted to glass surfaces like windows or film coverings such as on mobile phones. In addition, it could be adapted to greenhouses to help make the crops' light spectrum more specific, which would have a positive effect on the growth of vegetables.

Acknowledgments

We would like to express our deep and sincere gratitude to our supervisor, Mr. Khunthong Klaythong, and our special supervisor, Assoc. Prof. Voranuch Thongpool, for guiding and encouraging us to achieve this research.

Thank you to Dr. Samorn Pato, school principal of Princess Chulabhorn Science High School, for giving us permission to conduct this research as well as allowing us to use the school's facilities on this research.

Bibliography

Bacon, M., Bradley, S., & Nann, T. (2013). **Graphene Quantum Dots**. Particle &Amp; Particle Systems Characterization, 31(4), 415-428. https://doi.org/10.1002/ppsc.201300252

Chen, C. (2003). **Evaluation of Air Oven Moisture Content Determination Methods for Rough Rice**. Biosystems Engineering, 86(4), 447-457. https://doi.org/10.1016/j.biosystemseng.2003.08.010

Chen, C., Wang, F., Mao, C., Liao, W., & Hsieh, C. (2008). **Studies of chitosan: II. Preparation and characterization of chitosan/poly(vinyl alcohol)/gelatin ternary blend films**. International Journal Of Biological Macromolecules, 43(1), 37-42. https://doi.org/10.1016/j.ijbiomac.2007.09.005

Chuang, W. (2000). **The effect of acetic acid on the structure and filtration properties of poly(vinyl alcohol) membranes**. Journal Of Membrane Science, 172(1-2), 241-251. https://doi.org/10.1016/s0376-7388(00)00336-7

Crapper, G. (2012). **Powder Coatings**. Polymer Science: A Comprehensive Reference, 541-566. https://doi.org/10.1016/b978-0-444-53349-4.00279-x

Delgado-Sanchez, J. (2019). **Luminescent solar concentrators: Photo-stability analysis and long-term perspectives**. Solar Energy Materials And Solar Cells, 202, 110134. https://doi.org/10.1016/j.solmat.2019.110134

DeMerlis, C., & Schoneker, D. (2003). **Review of the oral toxicity of polyvinyl alcohol (PVA)**. Food And Chemical Toxicology, 41(3), 319-326. https://doi.org/10.1016/s0278-6915(02)00258-2

Diepens, M., & Gijsman, P. (2009). **Photostabilizing of bisphenol A polycarbonate by using UV-absorbers and self protective block copolymers based on resorcinol polyarylate blocks**. Polymer Degradation And Stability, 94(10), 1808-1813. https://doi.org/10.1016/j.polymdegradstab.2009.06.008

Ghebaur, A., Garea, S., & Iovu, H. (2012). **New polymer–halloysite hybrid materials—potential controlled drug release system**. International Journal Of Pharmaceutics, 436(1-2), 568-573. https://doi.org/10.1016/j.ijpharm.2012.07.014

Gu, J., Zhang, X., Pang, A., & Yang, J. (2016). **Facile synthesis and photoluminescence characteristics of blue-emitting nitrogen-doped graphene quantum dots**. Nanotechnology, 27(16), 165704. https://doi.org/10.1088/0957-4484/27/16/165704

Guo, Z., Zhang, D., Wei, S., Wang, Z., Karki, A., & Li, Y. et al. (2009). **Effects of iron oxide nanoparticles on polyvinyl alcohol: interfacial layer and bulk nanocomposites thin film**. Journal Of Nanoparticle Research, 12(7), 2415-2426. https://doi.org/10.1007/s11051-009-9802-z

Hasan, M., Gonzalez-Rodriguez, R., Ryan, C., Coffer, J., & Naumov, A. (2019). **Variation of Optical Properties of Nitrogen-doped Graphene Quantum Dots with Short/Mid/Long-wave Ultraviolet for the Development of the UV Photodetector**. ACS Applied Materials &Amp; Interfaces, 11(42), 39035-39045. https://doi.org/10.1021/acsami.9b10365

ITOH, Y., GU, H., SATOH, K., & KUTSUNA, Y. (2006). **EXPERIMENTAL INVESTIGATION ON AGEING BEHAVIORS OF RUBBERS USED FOR BRIDGE BEARINGS**. STRUCTURAL ENGINEERING / EARTHQUAKE ENGINEERING, 23(1), 17s-31s. https://doi.org/10.2208/jsceseee.23.17s

Kamoun, E., Chen, X., Mohy Eldin, M., & Kenawy, E. (2015). **Crosslinked poly(vinyl alcohol) hydrogels for wound dressing applications: A review of remarkably blended polymers**. Arabian Journal Of Chemistry, 8(1), 1-14. https://doi.org/10.1016/j.arabjc.2014.07.005

Limpan, N., Prodpran, T., Benjakul, S., & Prasarpran, S. (2012). **Influences of degree of hydrolysis and molecular weight of poly(vinyl alcohol) (PVA) on properties of fish myofibrillar protein/PVA blend films**. Food Hydrocolloids, 29(1), 226-233. https://doi.org/10.1016/j.foodhyd.2012.03.007

Liu, F., Jang, M., Ha, H., Kim, J., Cho, Y., & Seo, T. (2013). **Graphene Quantum Dots: Facile Synthetic Method for Pristine Graphene Quantum Dots and Graphene Oxide Quantum Dots: Origin of Blue and Green Luminescence (Adv. Mater. 27/2013)**. Advanced Materials, 25(27), 3748-3748. https://doi.org/10.1002/adma.201370175

Liu, M., Guo, B., Du, M., & Jia, D. (2007). **Drying induced aggregation of halloysite nanotubes in polyvinyl alcohol/halloysite nanotubes solution and its effect on properties of composite film**. Applied Physics A, 88(2), 391-395. https://doi.org/10.1007/s00339-007-3995-8

Maria, T., de Carvalho, R., Sobral, P., Habitante, A., & Solorza-Feria, J. (2008). **The effect of the degree of hydrolysis of the PVA and the plasticizer concentration on the color, opacity, and thermal and mechanical properties of films based on PVA and gelatin blends**. Journal Of Food Engineering, 87(2), 191-199. https://doi.org/10.1016/j.jfoodeng.2007.11.026

Marlina, P., & Adi Prasetya, H. (2017). **CHARACTERISTICS OF RUBBER SHEET WITH RAW MATERIAL OF COMPOSITE MODIFICATIONS - LATEX**. Jurnal Dinamika Penelitian Industri, 28(2), 112. https://doi.org/10.28959/jdpi.v28i2.3081

Mastalygina, E., Varyan, I., Kolesnikova, N., Gonzalez, M., & Popov, A. (2020). **Effect of Natural Rubber in Polyethylene Composites on Morphology, Mechanical Properties and Biodegradability**. Polymers, 12(2), 437. https://doi.org/10.3390/polym12020437

Mok, C., Ching, Y., Muhamad, F., Abu Osman, N., Hai, N., & Che Hassan, C. (2020). **Adsorption of Dyes Using Poly(vinyl alcohol) (PVA) and PVA-Based Polymer Composite Adsorbents: A Review**. Journal Of Polymers And The Environment, 28(3), 775-793. https://doi.org/10.1007/s10924-020-01656-4

Papaioannou, N., Titirici, M., & Sapelkin, A. (2019). **Investigating the Effect of Reaction Time on Carbon Dot Formation, Structure, and Optical Properties**. ACS Omega, 4(26), 21658-21665. https://doi.org/10.1021/acsomega.9b01798

Pryor, C. The Definitive Guide to ASTM D882 **- Tensile Testing of Thin Plastic Film. instron**. Retrieved 1 April 2022, from https://www.instron.com/en/testing-solutions/by-standard/astm/astm-d882?region=Global%20Site.

Purcell-Milton, F., & Gun'ko, Y. (2012). **Quantum dots for Luminescent Solar Concentrators**. Journal Of Materials Chemistry, 22(33), 16687. https://doi.org/10.1039/c2jm32366d

Qu, D., Zheng, M., Zhang, L., Zhao, H., Xie, Z., & Jing, X. et al. (2014). **Formation mechanism and optimization of highly luminescent N-doped graphene quantum dots**. Scientific Reports, 4(1). https://doi.org/10.1038/srep05294

Repacholi, M. (2000). **Global Solar UV Index**. Radiation Protection Dosimetry, 91(1), 307-311. https://doi.org/10.1093/oxfordjournals.rpd.a033226

SHI, H., ZHAO, Q., ZHOU, C., & JIA, N. (2022). **Nitrogen and sulfur co-doped carbon quantum dots as fluorescence sensor for detection of lead ion**. Chinese Journal Of Analytical Chemistry, 50(2), 63-68. https://doi.org/10.1016/j.cjac.2021.09.010

Shi, R., Bi, J., Zhang, Z., Zhu, A., Chen, D., & Zhou, X. et al. (2008). **The effect of citric acid on the structural properties and cytotoxicity of the polyvinyl alcohol/starch films when molding at high temperature**. Carbohydrate Polymers, 74(4), 763-770. https://doi.org/10.1016/j.carbpol.2008.04.045

Silva, M., Claro, P., da Silva, J., Scaloppi Júnior, E., de Souza Gonçalves, P., Martins, M., & Mattoso, L. (2021). **Evaluation of the physicochemical properties of natural rubber from Hevea brasiliensis clones**. Industrial Crops And Products, 171, 113925. https://doi.org/10.1016/j.indcrop.2021.113925

Sk, M., Ananthanarayanan, A., Huang, L., Lim, K., & Chen, P. (2014). **Revealing the tunable photoluminescence properties of graphene quantum dots**. J. Mater. Chem. C, 2(34), 6954-6960. https://doi.org/10.1039/c4tc01191k

Appendix

		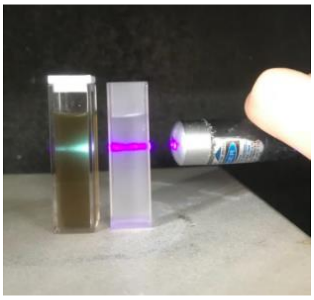
A.1 Measuring chemical	A.2 Teflon lined autoclave in oven	A.3 comparing T4 with water
		
A.4 UV/VIS spectrophotometer	A.5 Measuring fluorescent spectrum	A.6 Mixture of TS6 and PVA
	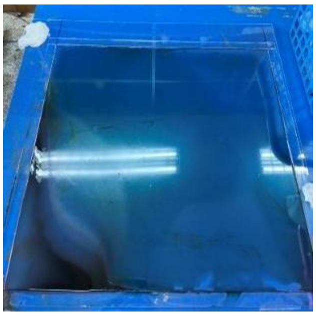	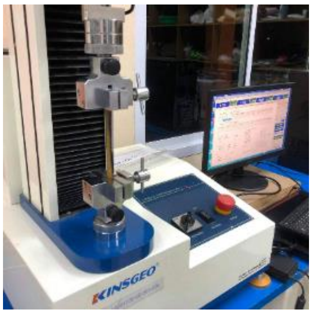
A.7 Preparing of roof's mold from acrylic	A.8 Forming of P-UV	A.9 Tensile tester
		
A.10 Testing physical propertie of P-IR and P-UV	A.11 P-IR sample for testing physical properties	A.12 Prototype of rubber drying chamber

【評語】160040

This is an interesting and creative idea to solve the problem of rubber drying chamber. The idea of using Nitrogen doping QDs is good; however，the structure of the produced materials can be more detailly studied. It would be even better to talk about the possibility of scale-up production，perhaps compare with the performance of currently used materials.